Supplementary Information

Interfacial Chemistry Modulation of Zn Anode via EMImI Ionic Liquid Additive for Stable Aqueous Zinc-Ion Batteries

Yulong Wu[1], Luyao Wen[1], Shiqiang Wei[1], Jialin Shi[1], Quan Zhou[1], Qian Zhou[1], Wei Jiang[1], Xiaojun Wu[2], Peter Joseph Chimtali[1, 3], Qiang Chi[4], Changda Wang[1*], Li Song[1, 5*]*

[1]National Synchrotron Radiation Laboratory, State Key Laboratory of Precision and Intelligent Chemistry, University of Science and Technology of China, Hefei, Anhui 230029, China

[2]School of Chemistry and Material Sciences, University of Science and Technology of China, Hefei, Anhui 230026, China

[3]Department of Chemistry and Chemical Engineering, School of Natural and Applied Sciences, University of Malawi, P.O. Box 280, Zomba, Malawi

[4]State Key Laboratory of Oil and Gas Equipment, CNPC Tubular Goods Research Institute, Xi'an, Shaanxi 710077, China

[5]Zhejiang Institute of Photonelectronics, Jinhua, Zhejiang 321004, China

[*]Email: Qiang Chi (chiq@cnpc.com.cn) ; Changda Wang (wchda@ustc.edu.cn); Li Song (song2012@ustc.edu.cn)

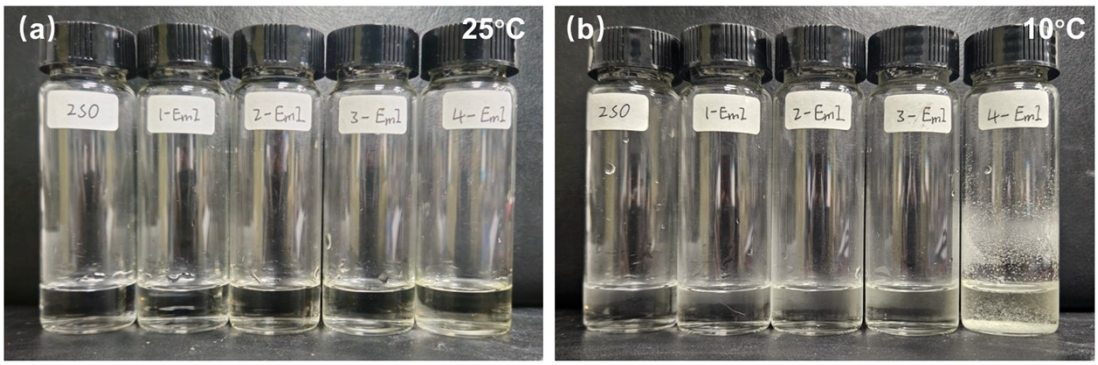

Figure S1. Digital photos of the 2 M $ZnSO_4$ electrolytes with 0 M, 0.1 M, 0.2 M, 0.3 M, and 0.4 M EMImI (from left to right) at (a) 25 ℃ and (b) 10 ℃.

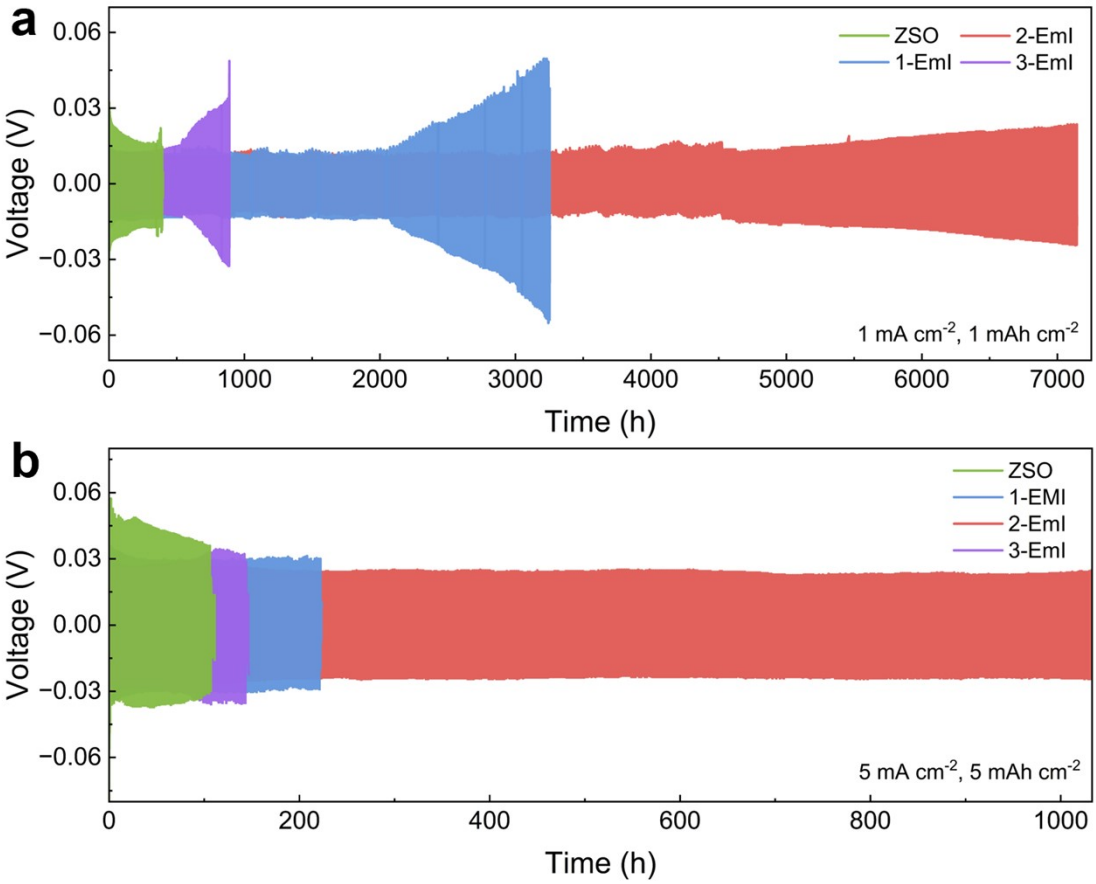

Figure S2. Cycling performance of Zn//Zn symmetric cells in 2 M $ZnSO_4$ electrolytes with 0.1 M, 0.2 M, and 0.3 M EMImI at (a) 1 mA cm^{-2} with a capacity of 1 mAh cm^{-2} and (b) 5 mA cm^{-2} with a capacity of 5 mAh cm^{-2}.

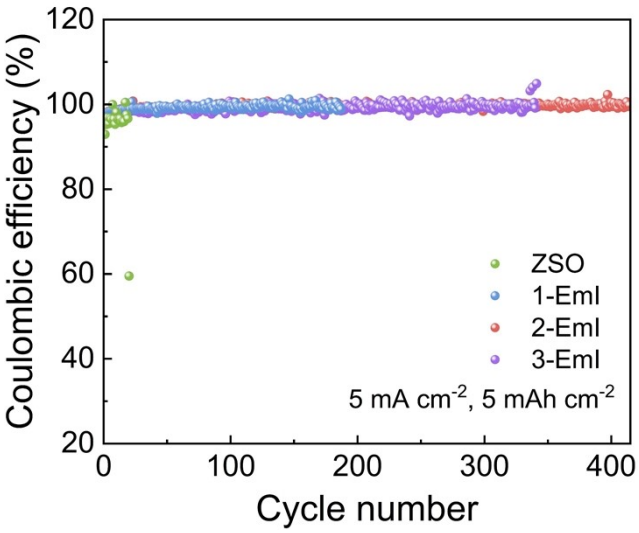

Figure S3. Coulombic efficiency of Zn//Cu asymmetric cells at 5 mA cm^{-2} and 5 mAh cm^{-2} in various electrolytes.

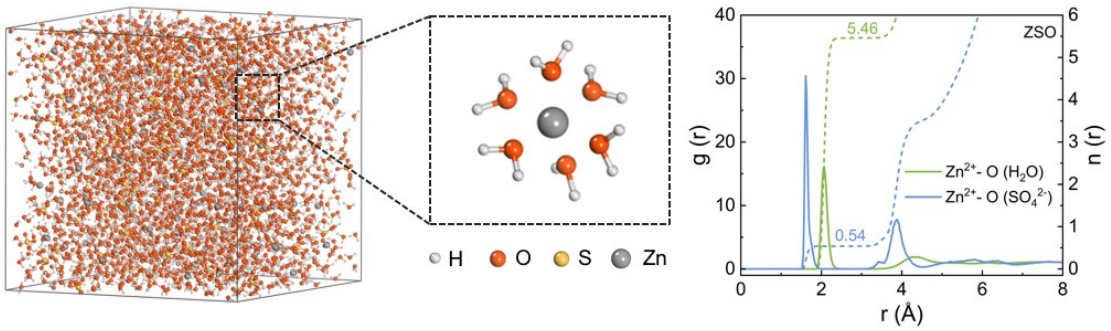

Figure S4. 3D snapshot, RDF and CN of ZSO electrolyte from MD simulations.

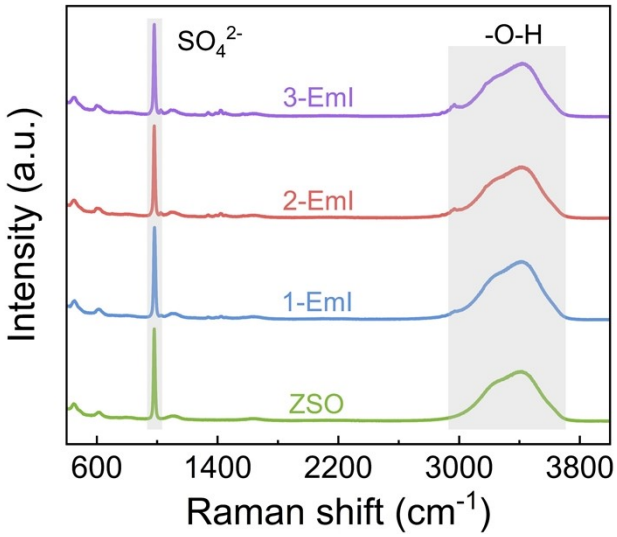

Figure S5. Raman spectra of different electrolytes.

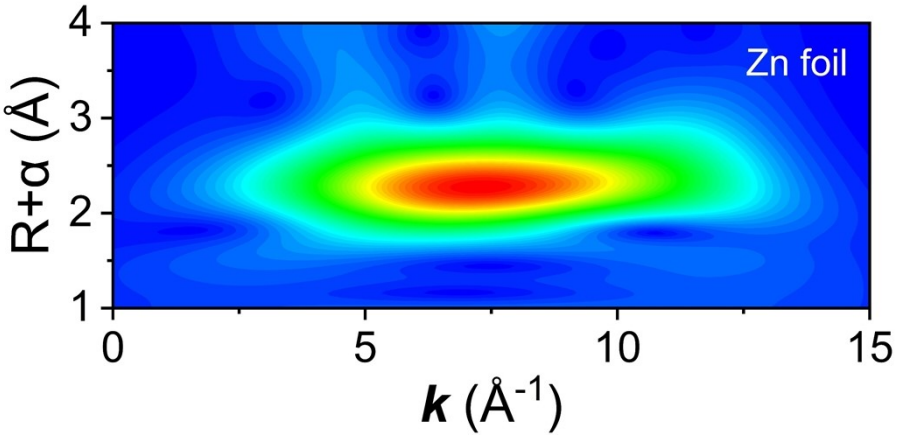

Figure S6. Wavelet transforms of Zn K-edge XANES spectra of Zn foil.

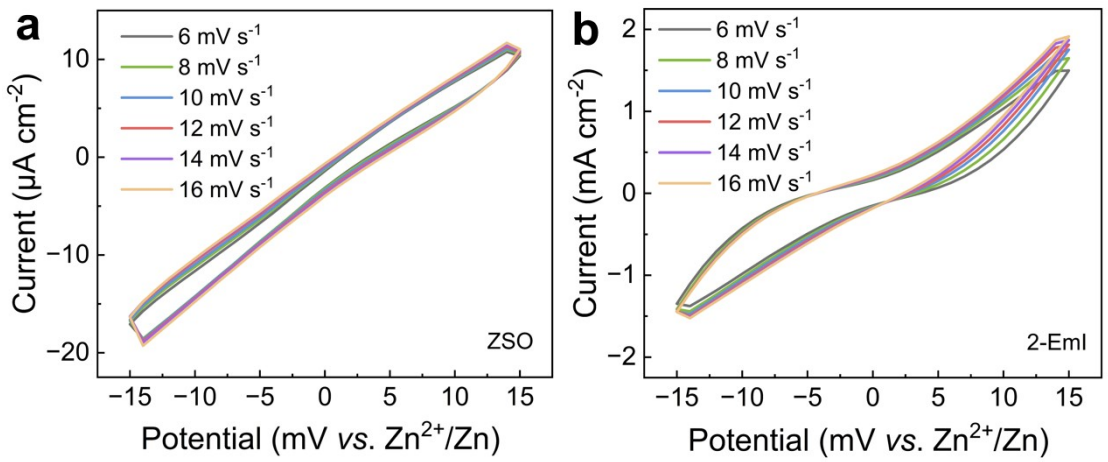

Figure S7. CV curves of Zn//Zn symmetric cells at different scan rates in (a) ZSO and (b) 2-EmI electrolytes.

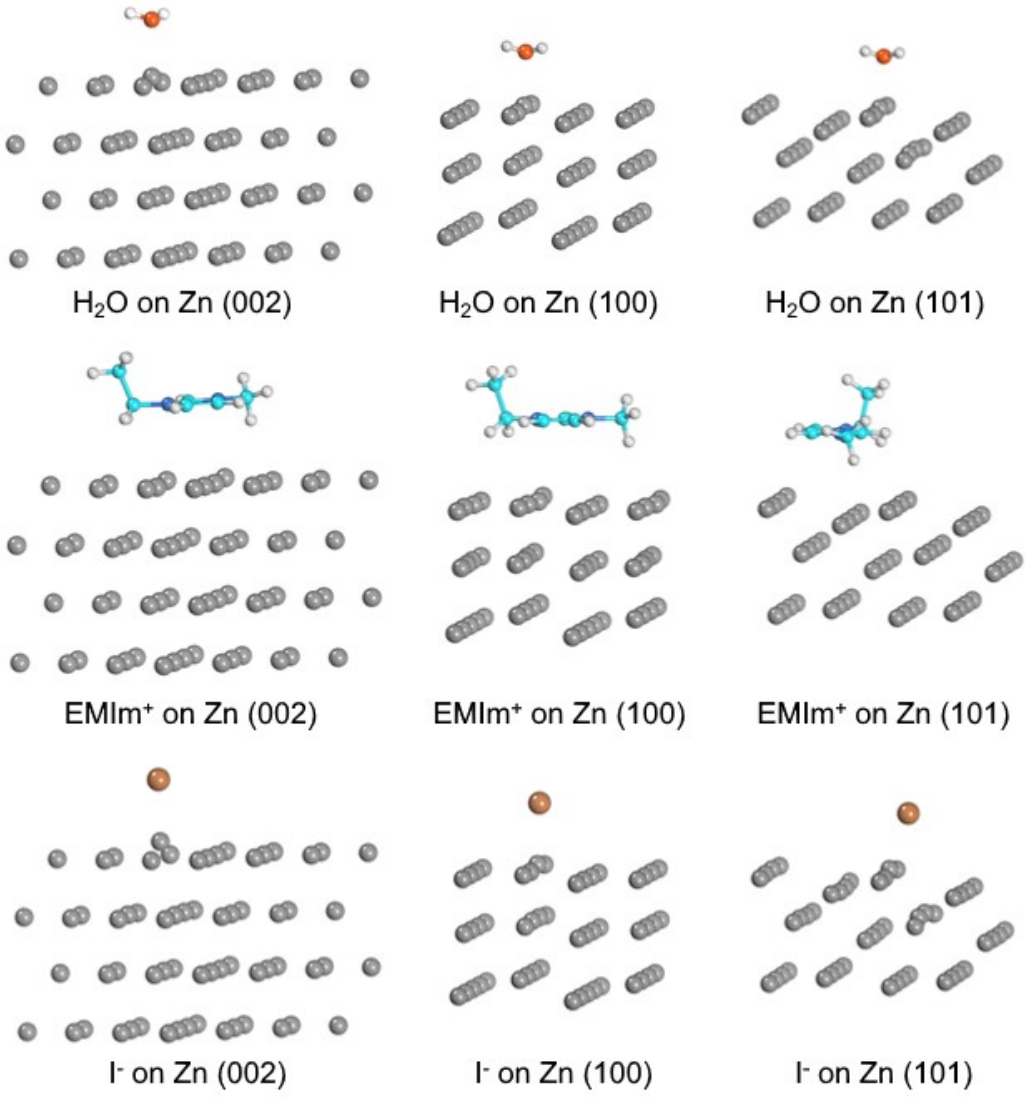

Figure S8. Adsorption models of H_2O, $EMIm^+$, and I^- on the Zn anode

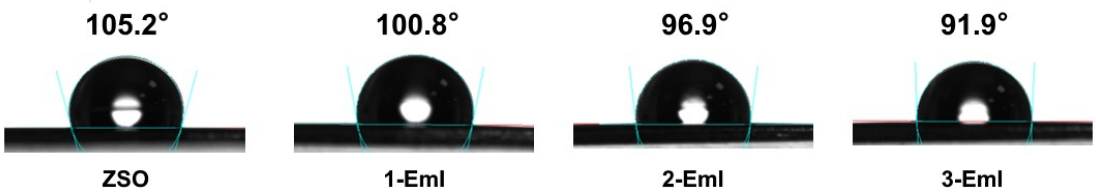

Figure S9. Contact angles of the electrolytes with 0.1 M, 0.2 M, and 0.3 M EMImI on Zn foil.

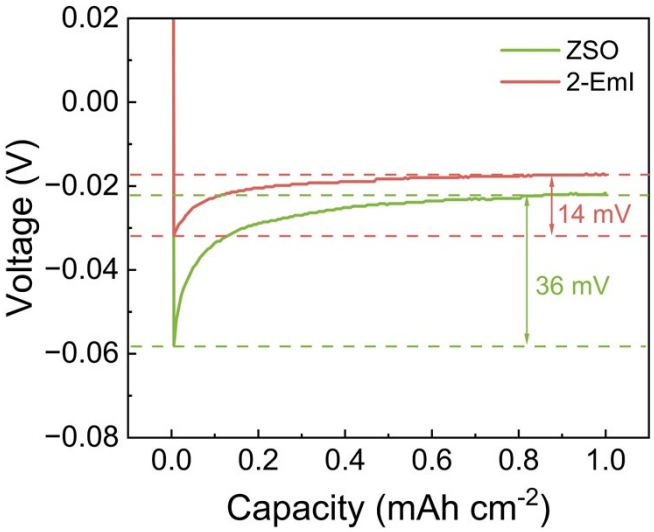

Figure S10. Initial Zn nucleation overpotentials on Cu foil of Zn//Cu asymmetric cells at 1 mA cm^{-2} and 1 mAh cm^{-2} in different electrolytes.

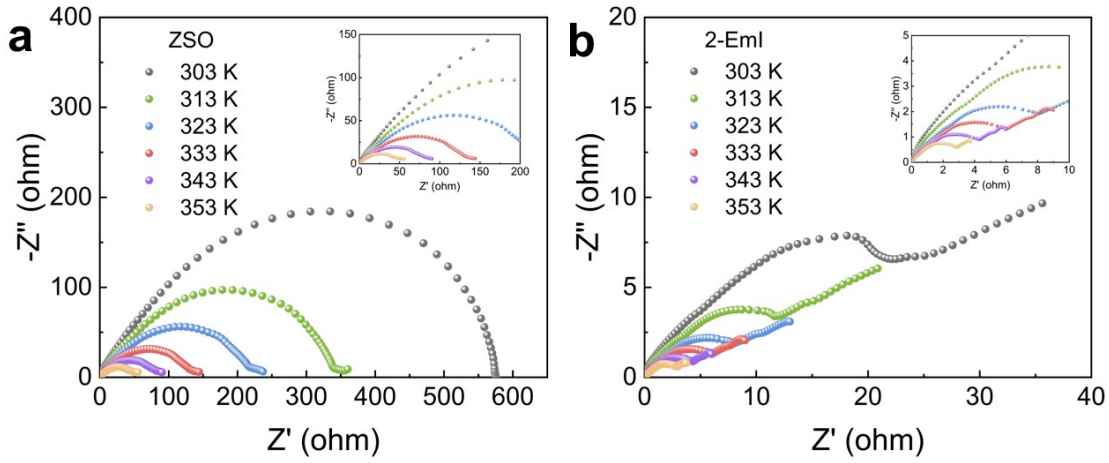

Figure S11. EIS spectra of Zn//Zn symmetric cells at different temperatures in (a) ZSO and (b) 2-EmI electrolytes.

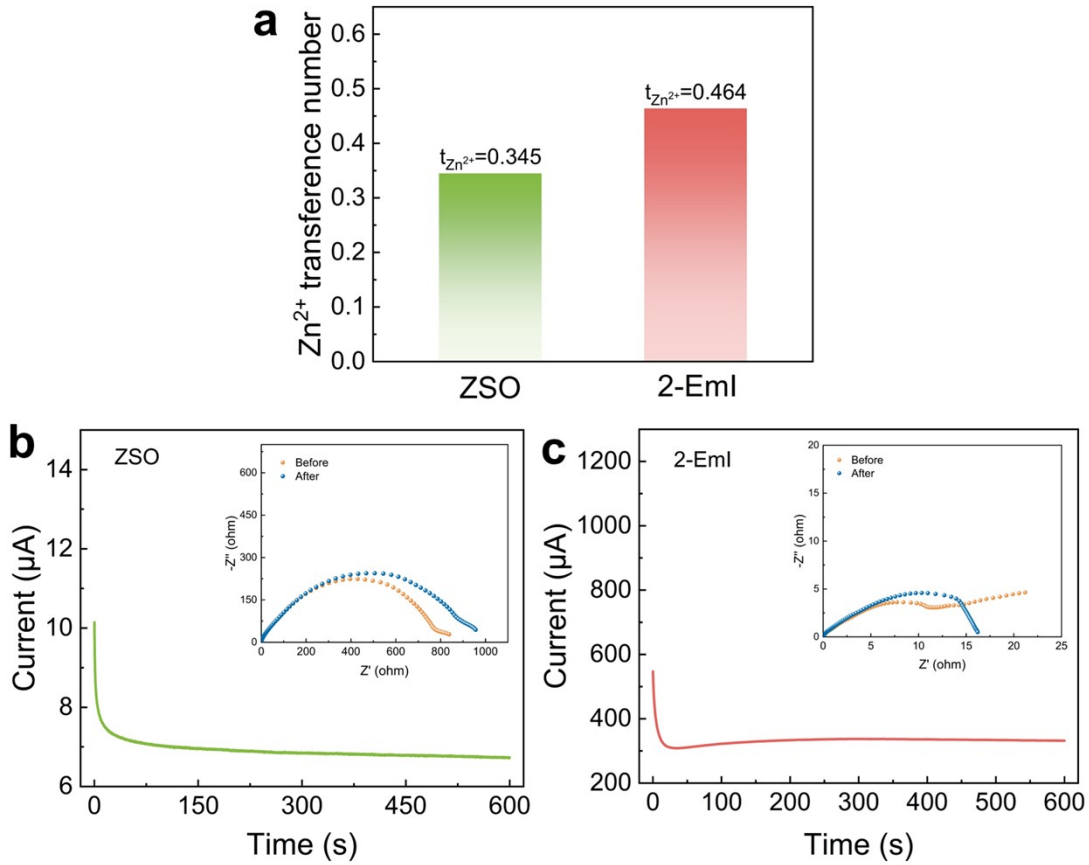

Figure S12. (a) Zn^{2+} transference number of Zn//Zn symmetric cells. Chronoamperometry curves and EIS spectra before and after polarization of symmetric Zn//Zn cells in (b) ZSO and (c) 2-EmI electrolytes.

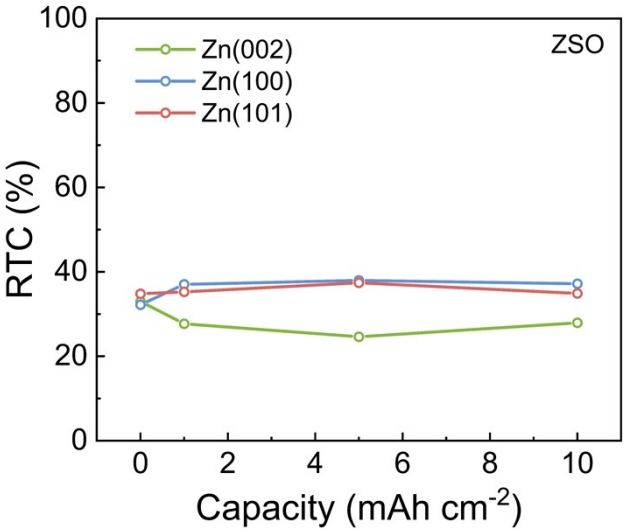

Figure S13. RTCs of Zn electrodes with different Zn deposition capacities in ZSO electrolyte.

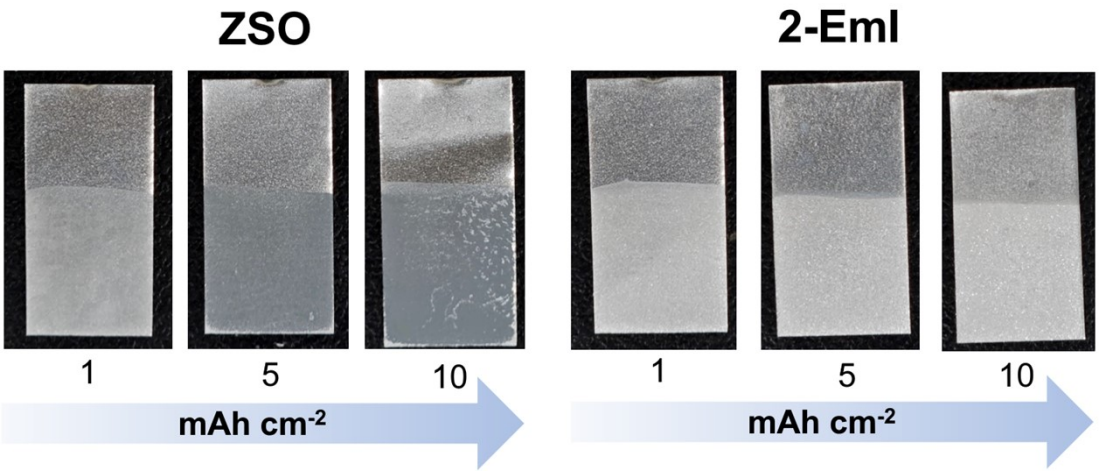

Figure S14. Digital photos of Zn electrodes with different Zn deposition capacities at 10 mA cm^{-2} in ZSO and 2-EmI electrolytes.

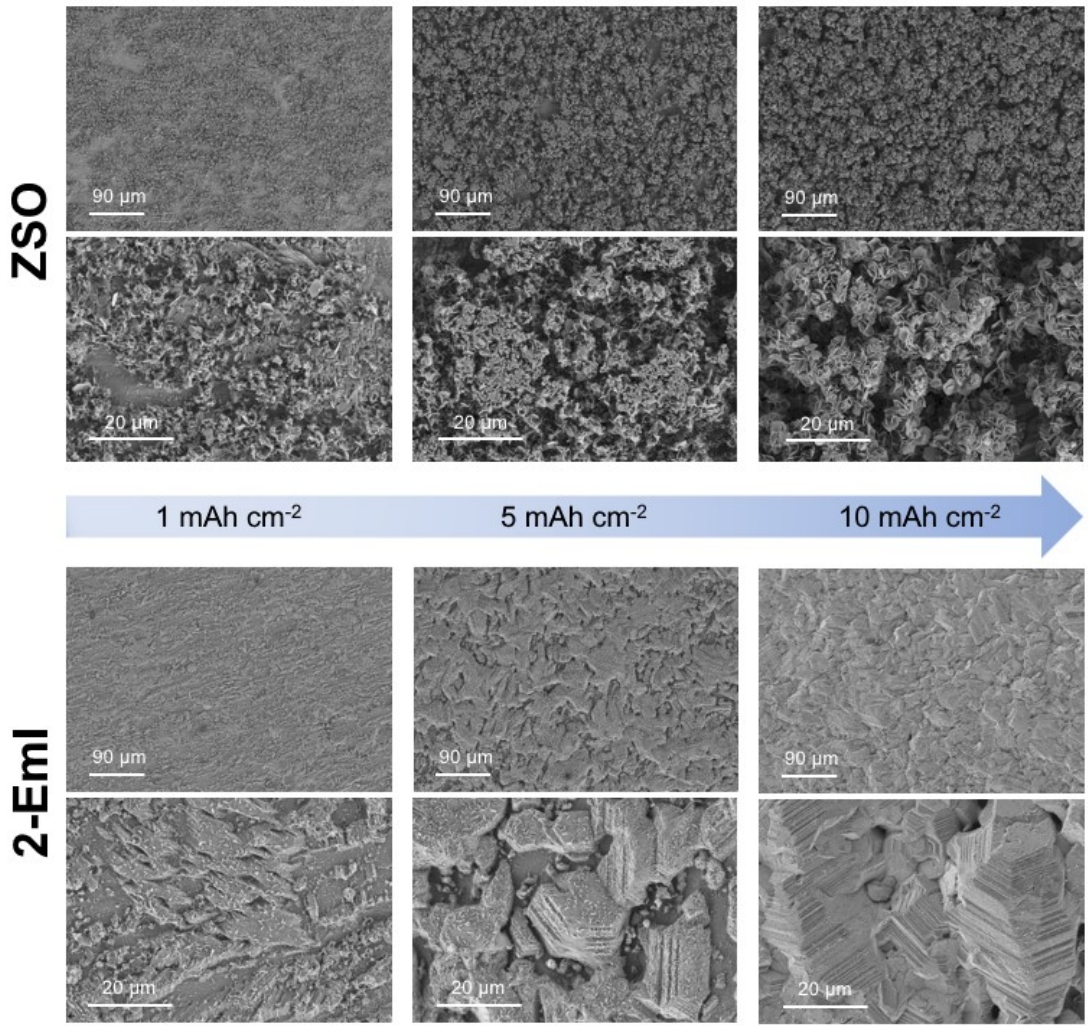

Figure S15. SEM images of Zn electrodes with different Zn deposition capacities at 10 mA cm^{-2} in ZSO and 2-EmI electrolytes.

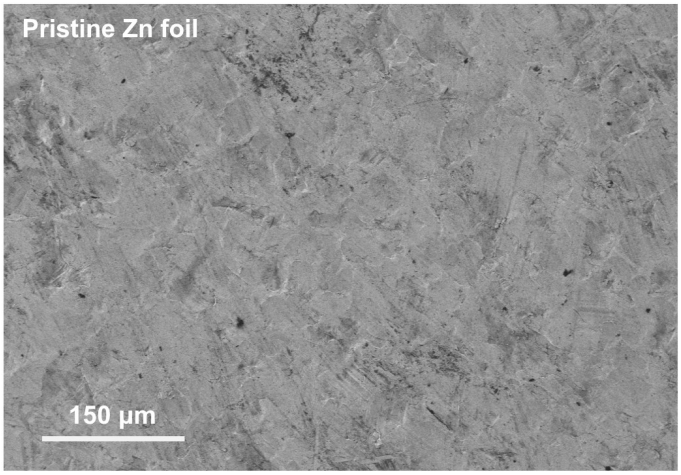

Figure S16. SEM image of pristine Zn foil.

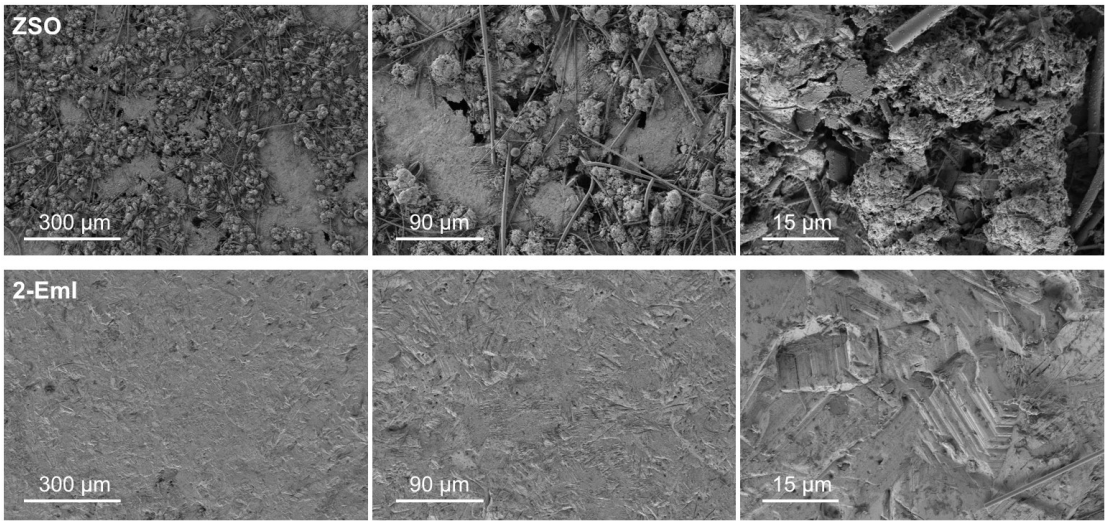

Figure S17. SEM images of Zn electrodes after 50 cycles at 1 mA cm^{-2} and 1 mAh cm^{-2} in ZSO and 2-EmI electrolytes.

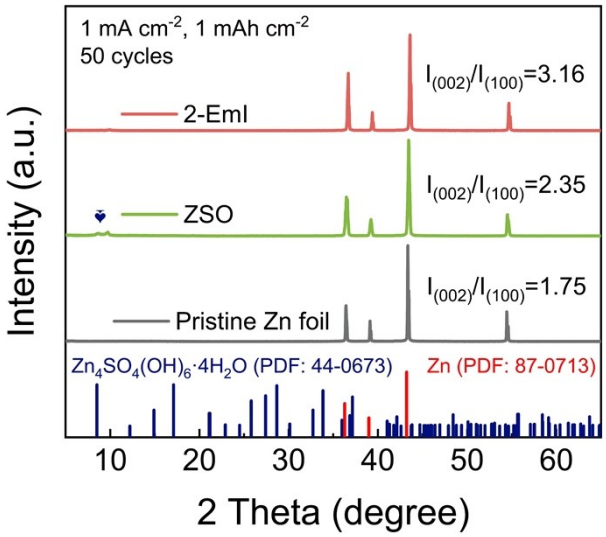

Figure S18. XRD patterns of Zn anodes after 50 cycles at 1 mA cm^{-2} and 1 mAh cm^{-2}.

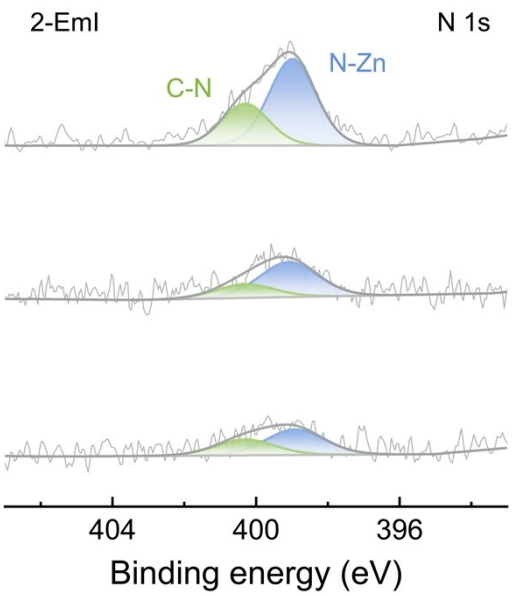

Figure S19. XPS depth profiles of N 1s for the cycled Zn electrodes in 2-EmI electrolyte.

$$SO_4^{2-} + H_2O + 2e^- \rightarrow SO_3^{2-} + 2OH^- \quad (1)$$

$$SO_3^{2-} + 3H_2O + 6e^- \rightarrow S^{2-} + 6OH^- \quad (2)$$

$$Zn^{2+} + SO_3^{2-} \rightarrow ZnSO_3 \quad (3)$$

$$Zn^{2+} + S^{2-} \rightarrow ZnS \quad (4)$$

$$Zn + 4OH^- \leftrightarrow Zn(OH)_4^{2-} + 2e^- \quad (5)$$

$$Zn(OH)_4^{2-} \leftrightarrow ZnO + H_2O + 2OH^- \quad (6)$$

$$Zn^{2+} + CO_3^{2-} \rightarrow ZnCO_3 \quad (7)$$

$$Zn^{2+} + 2I^- \rightarrow ZnI_2 \quad (8)$$

Figure S20. The possible chemical reactions for the formation of inorganic components in the SEI.

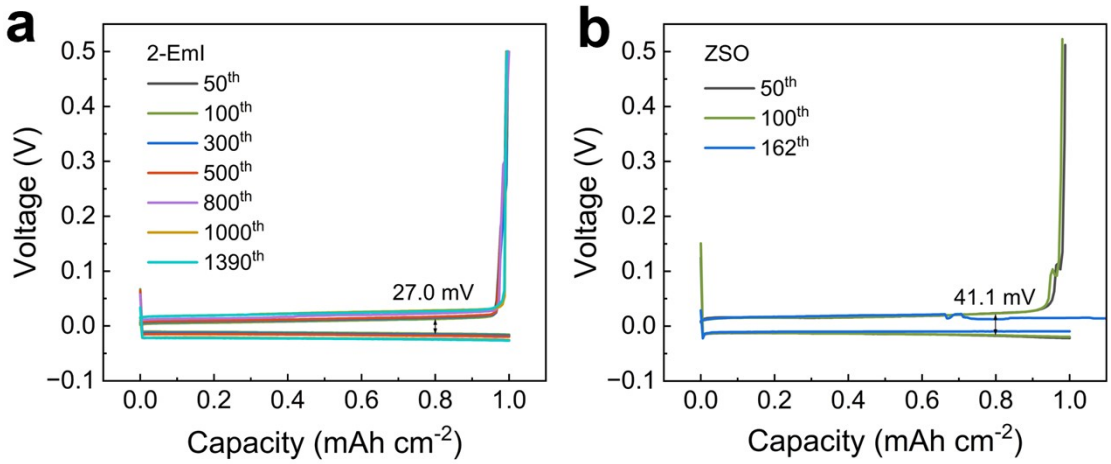

Figure S21. Voltage profiles of Zn//Cu asymmetric cells at various cycles in (a) 2-EmI and (b) ZSO electrolyte.

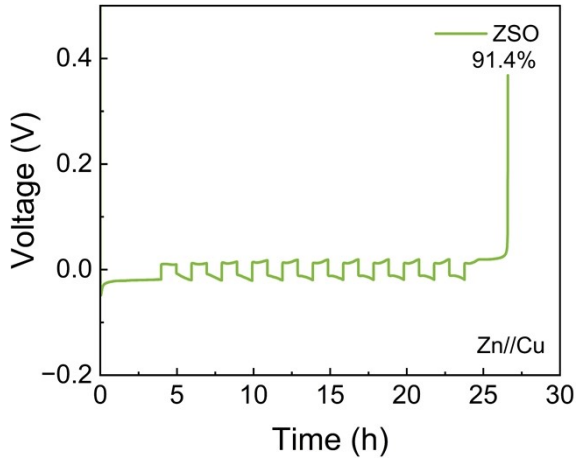

Figure S22. Average coulombic efficiency measurements in Zn//Cu asymmetric cells using ZSO electrolyte.

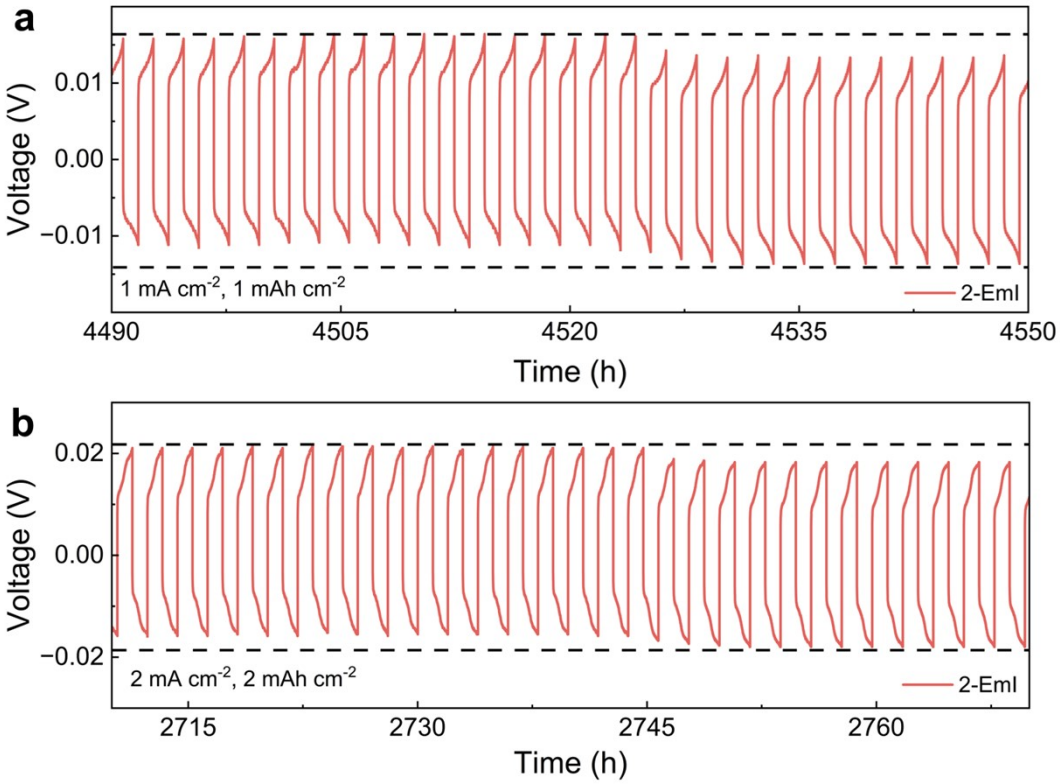

Figure S23. Partial cycling voltage curves of Zn//Zn symmetric cells with 2-EmI electrolyte at (a) 1 mA cm^{-2} and 1 mAh cm^{-2}, (b) 2 mA cm^{-2} and 2 mAh cm^{-2}.

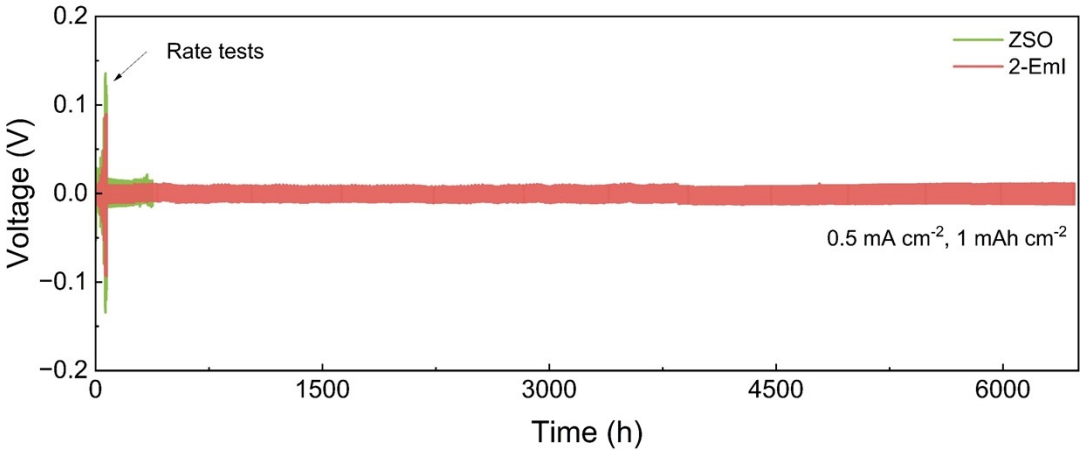

Figure S24. Cycling performance of Zn//Zn symmetric cells at 0.5 mA cm^{-2} and 1 mAh cm^{-2} after rate tests.

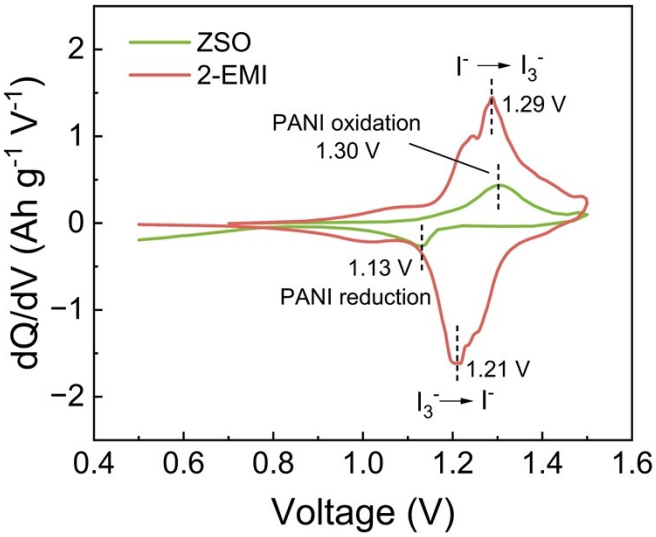

Figure S25. Differential capacity curves of Zn//PANI cells.

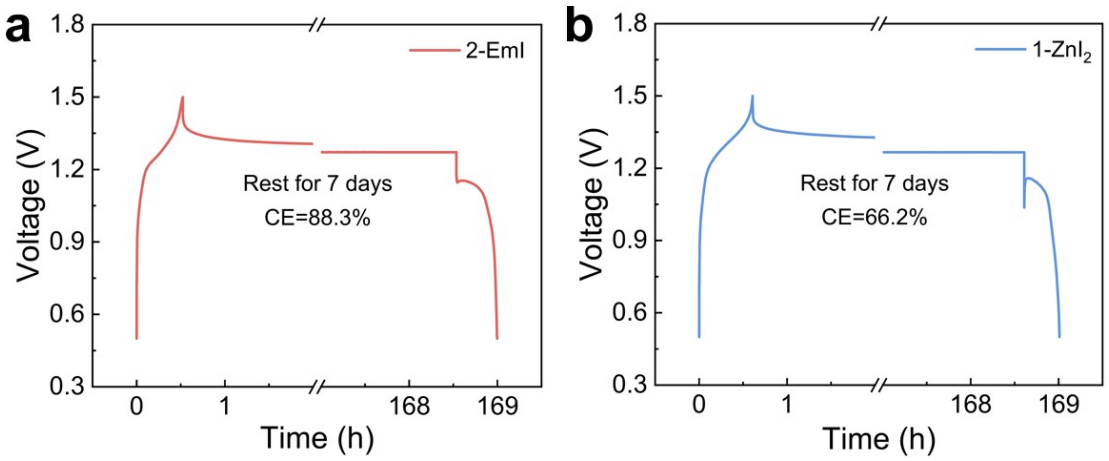

Figure S26. The self-discharge curves of Zn//PANI full cells in 2-EmI and 1-ZnI_2 electrolytes.

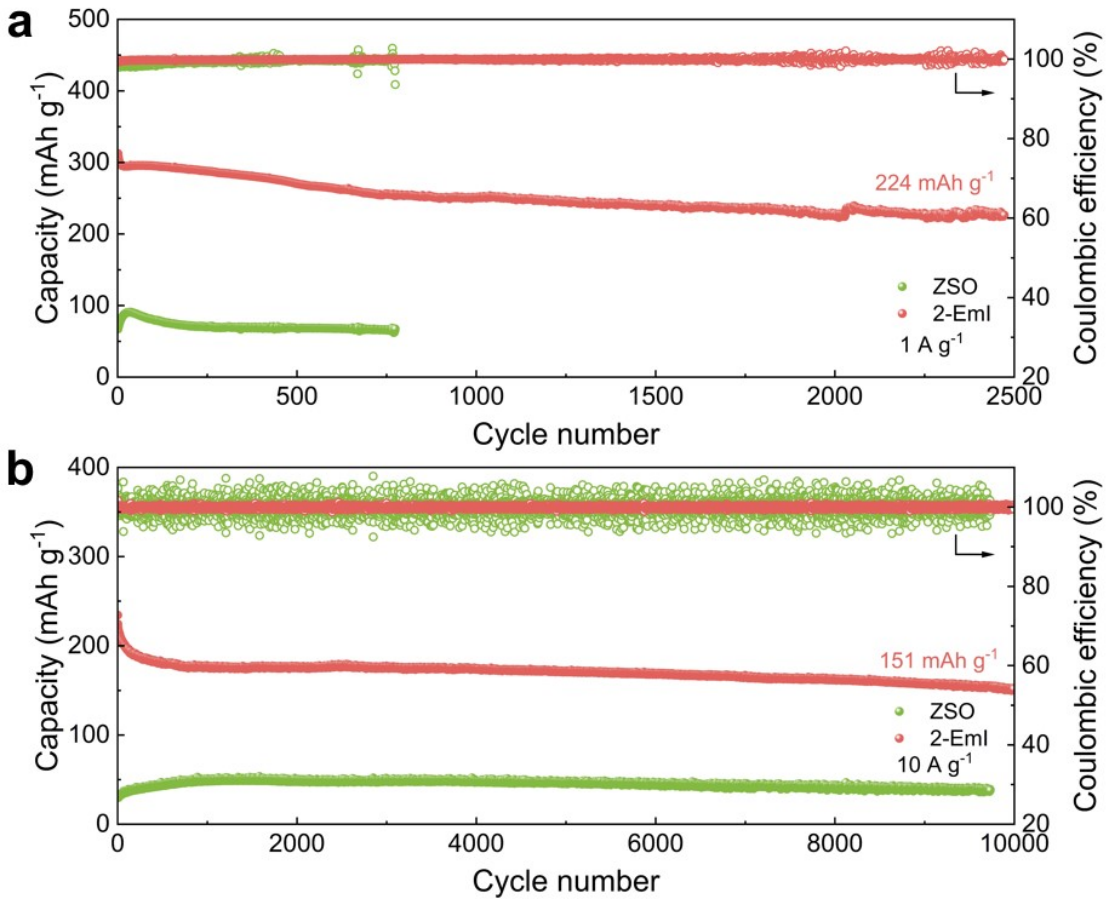

Figure S27. Cycling performance of Zn//PANI full cells at (a) 1 A g^{-1} and (b) 10 A g^{-1}.

Table S1. Comparison of symmetric cells lifespan in this work with previous studies.

Electrolyte	Current density (mA cm^{-2})	Capacity (mAh cm^{-2})	Lifespan (h)	Ref.
0.2 M EMImI + 2 M $ZnSO_4$	**1**	**1**	**7100**	**This work**
	2	**2**	**5100**	
	5	**5**	**1030**	
1% $[BMIM]PF_6$ + 2 M $ZnSO_4$	1	1	800	[1]
0.2 M [EMIM][OAc] + 2 M $ZnSO_4$	1	0.5	3000	[2]
0.05 M [BMIM]Br + 2 M $ZnSO_4$	1	1	2700	[3]
0.025 M $BMIHSO_4$ + 2 M $ZnSO_4$	2	2	3600	[4]
6 M MGM[TFSI] + 2 M $Zn(OTf)_2$	1	1	2000	[5]
3.6 M [EMIM]OTf + 2 M $Zn(OTf)_2$	2	2	3400	[6]
10% HEI + 2 M $ZnSO_4$	1	1	4200	[7]
0.1 M NDSB + 2 M $ZnSO_4$	1	1	2500	[8]
0.14 mM EC + 1 M $ZnSO_4$	1	1	750	[9]
0.01 M TA-Na + 1 M $ZnSO_4$	0.5	0.25	1500	[10]
3 mM DTPA + 2 M $ZnSO_4$	1	1	3300	[11]
0.1 M AOT + 1 M $Zn(OTf)_2$ (solvent: NB_{volume}:$water_{volume}$ = 6:4)	1	1	5500	[12]
2% MPC + 2 M $ZnSO_4$	1	1	5000	[13]

0.3% C5SeCN + 2 M $ZnSO_4$	1	1	4500	[14]
0.04 M TFMI + 2 M $ZnSO_4$	1	1	2100	[15]

References

1. C. Shen, Y. Zhang, X. Li, P. Guo, X. Zeng, K. Ni, R. Cao, Z. Wang, Z. Wang and L. Qin, *J. Mater. Chem. A*, 2025, **13**, 2174-2186.
2. T. Xiao, J. L. Yang, B. Zhang, J. Wu, J. Li, W. Mai and H. J. Fan, *Angew. Chem. Int. Ed.*, 2024, **63**, e202318470.
3. Y. Lv, C. Huang, M. Zhao, M. Fang, Q. Dong, W. Tang, J. Yang, X. Zhu, X. Qiao, H. Zheng, C. Sun, L. Zheng, M. Zheng, Y. Xu and J. Lu, *J. Am. Chem. Soc.*, 2025, **147**, 8523-8533.
4. Y. X. Song, J. Wang, X. B. Zhong, Y. H. Zhang, K. Wang, X. H. Guo, H. J. Guo, G. P. Lei, H. T. Liu, G. K. Wang, P. G. Ji, X. Zhang, U. Khalilov, J. F. Liang and R. Wen, *J. Colloid Interface Sci.*, 2024, **665**, 711-719.
5. S. Li, M. Xu, K. Chen, Q. Wu, Y. Li, C. Xie, Y. Li, Q. Xu, J. Huang and H. Xie, *J. Colloid Interface Sci.*, 2025, **678**, 934-947.
6. C. Liu, W. Xu, L. Zhang, D. Zhang, W. Xu, X. Liao, W. Chen, Y. Cao, M. C. Li, C. Mei and K. Zhao, *Angew. Chem. Int. Ed.*, 2024, **63**, e202318063.
7. J. Chen, G. Ou, P. Liu, W. Fan, B. Li, Z. Hu, Z. Wen, Y. Zhang, Y. Tang, X. Liu, M. Ye and C. C. Li, *Angew. Chem. Int. Ed.*, 2024, **64**, e202414166.
8. C. Jiang, M. Li, J. Fan, X. Zhu, C. Song, Z. Li, G. Xu, F.-H. Du, H. Wang, M. Wu, C. Pei, H. Fu and G. Wang, *Nano Energy*, 2025, **142**, 111178.
9. K. Wang, Y. Luo, H. Zhan, X. X. Liu and X. Sun, *ACS Nano*, 2024, **18**, 27672-27682.
10. J. Wan, R. Wang, Z. Liu, L. Zhang, F. Liang, T. Zhou, S. Zhang, L. Zhang, Q. Lu, C. Zhang and Z. Guo, *ACS Nano*, 2023, **17**, 1610-1621.
11. H. Zhang, T. Shui, W. Zhang and Z. Sun, *Energy Storage Mater.*, 2024, **71**, 103595.
12. Y. Ding, D. Huang, Y. Wang, X. Zhao, R. Han, M. Tang, B. Li, D. Zhou and F. Kang, *Adv. Mater.*, 2025, **37**, 2419221.
13. B. Wang, C. Guan, Q. Zhou, Y. Wang, Y. Zhu, H. Bian, Z. Chen, S. Zhang, X. Tan, B. Luo, S. Tang, X. Meng and C. Zhang, *Nano-Micro Lett.*, 2025, **17**, 314.
14. R. Han, T. Jiang, Z. Wang, R. Xue, X. Liu, Y. Tang, Z. Qi and Y. Ma, *Adv. Funct. Mater.*, 2024, **35**, 2412255.
15. M. Peng, Z. Liu, M. Hou, R. Zhang, M. Cheng, J. Yu, Y. Feng, P. Jiao, T. Zhang, Z. Zhang, X. Chen, Z. Hu and K. Zhang, *Angew. Chem. Int. Ed.*, 2025, **64**, e202501702.